


WIND TUNNEL RESULTS OF THE HIGH-SPEED NLF(1)-0213 AIRFOIL

William G. Sewall, Robert J. McGhee,  
David E. Hahne, and Frank L. Jordan, Jr.  
NASA Langley Research Center  
Hampton, Virginia



## ABSTRACT

Wind tunnel tests have been conducted to evaluate a natural laminar-flow airfoil designed for the high-speed jet aircraft in general aviation (ref. 1). The airfoil, designated as the HSNLF(1)-0213, has been tested in two-dimensional wind tunnels to investigate the performance of the basic airfoil shape. A three-dimensional wing designed with this airfoil and a high-lift flap system is also being evaluated with a full-size, half-span model.

## OUTLINE

The two-dimensional tests include low-speed tests in the Langley Low-Turbulence Pressure Tunnel (LTPT) at Mach numbers ranging from 0.10 to 0.30 to determine the extent of laminar flow possible at low speeds and also to measure the maximum lift of the basic airfoil (figure 1). The low-turbulence pressure tunnel is ideally suited for both of these items because of excellent flow quality and a unique force balance specifically designed for high-lift airfoils.

The high-speed characteristics were investigated in the Langley 6- by 28-Inch Transonic Tunnel to examine the cruise and climb performance at Mach numbers from 0.5 to 0.78.

The three-dimensional wing design has been recently tested in the Langley 30- by 60-Foot Tunnel with a half-span model that includes both a slotted flap and a fuselage shape. This investigation was conducted to determine the maximum lift for the flap system and to survey the boundary-layer characteristics at spanwise stations.

- 2-D tests, low speed, LTPT,  $M = .1 - .3$ 
  - Laminar flow
  - Maximum lift
- High speed test, 6 × 28 T.T.,  $M = .5 - .78$ 
  - Cruise/climb performance
- 3-D tests in 30 × 60
  - Full-scale semi-span model
  - Actual flap system

Figure 1

## AIRFOIL PROFILE

The shape of the HSNLF(1)-0213 airfoil shown in figure 2 represents a 13-percent thickness ratio which is designed for a cruise Mach number of 0.70, cruise lift coefficient of 0.26, and chord Reynolds number of 11 million.

These conditions allow laminar boundary layers back to 55-percent chord on the upper surface and 65-percent chord on the lower surface.

$$M = 0.7, c_l = 0.26, R = 11 \text{ million}$$

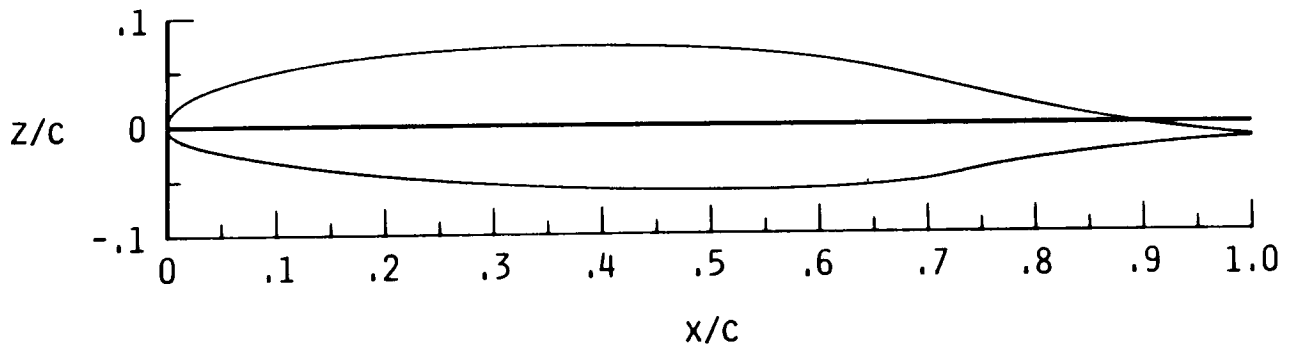


Figure 2

## LOW-SPEED TESTS IN LTPT

The low-speed, two-dimensional airfoil tests were conducted in LTPT with a solid model supported by an external force balance (figure 3a) connected to the tunnel sidewalls. This balance provides the lift and pitching moment while drag measurements are determined from a wake survey probe, which is shown behind the model in figure 3b.

Boundary layers on the surfaces of the model were assessed with hot-film gages to determine laminar, transitional, or turbulent flows.

An estimation of the high-lift capability with a simple flap system was provided with a trailing-edge split flap that appears on the model lower surface in figure 3b. This split flap was deflected 60 degrees in a similar manner to airfoil experiments described in ref. 2.

- Solid model
- Force balance for lift and pitching-moment
- Wake survey probe for drag
- Hot-film gages to assess boundary layers
- Simulated split flap

Figure 3a

ORIGINAL PAGE  
BLACK AND WHITE PHOTOGRAPH

**MODEL INSTALLATION IN LTPT**

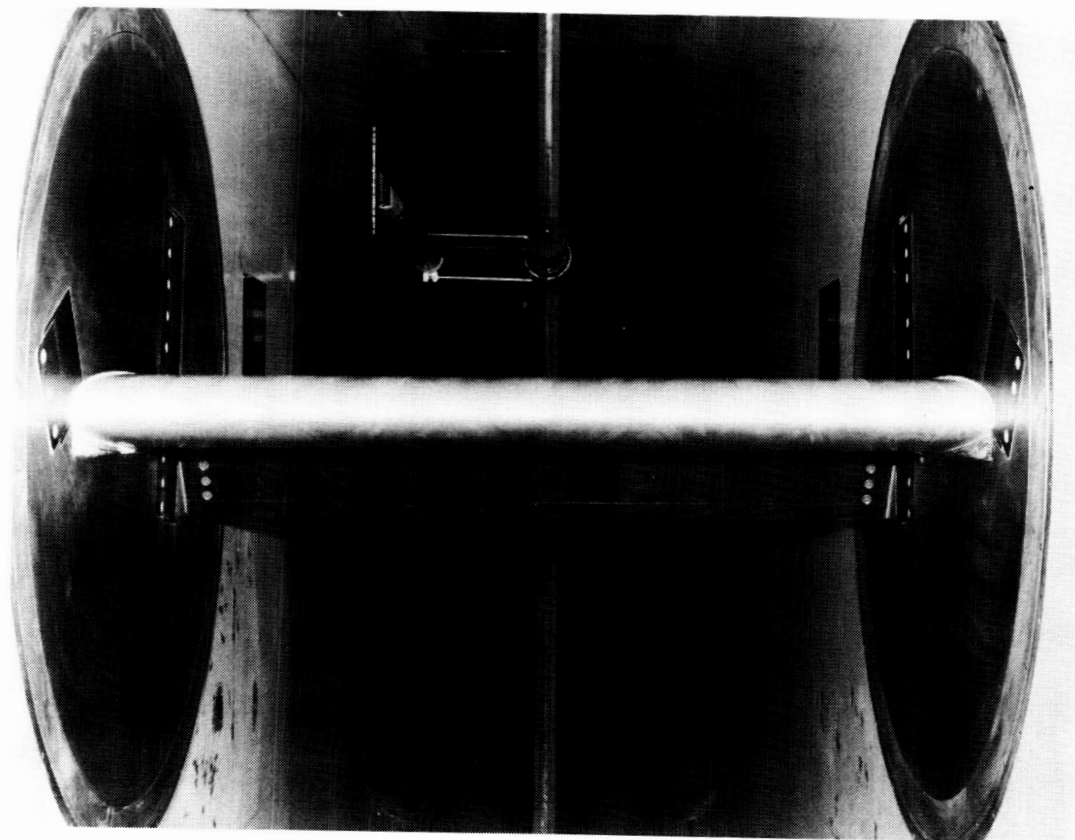


Figure 3b

~~ORIGINAL PAGE IS  
OF POOR QUALITY~~

## MINIMUM DRAG

The two-dimensional, low-speed tests were conducted with both smooth model surfaces and fixed transition from thin spanwise strips of carborundum at 5-percent chord on the upper and lower surfaces. The minimum drag from these two surface conditions is shown in figure 4 in variation with the Reynolds number. The difference in drag levels is approximately 0.0040 to 0.0045 in drag coefficient values, which is due to the extensive laminar boundary layers on the smooth model.

For the low-speed tests, minimum drag occurred at lift-coefficient values of approximately 0.20.

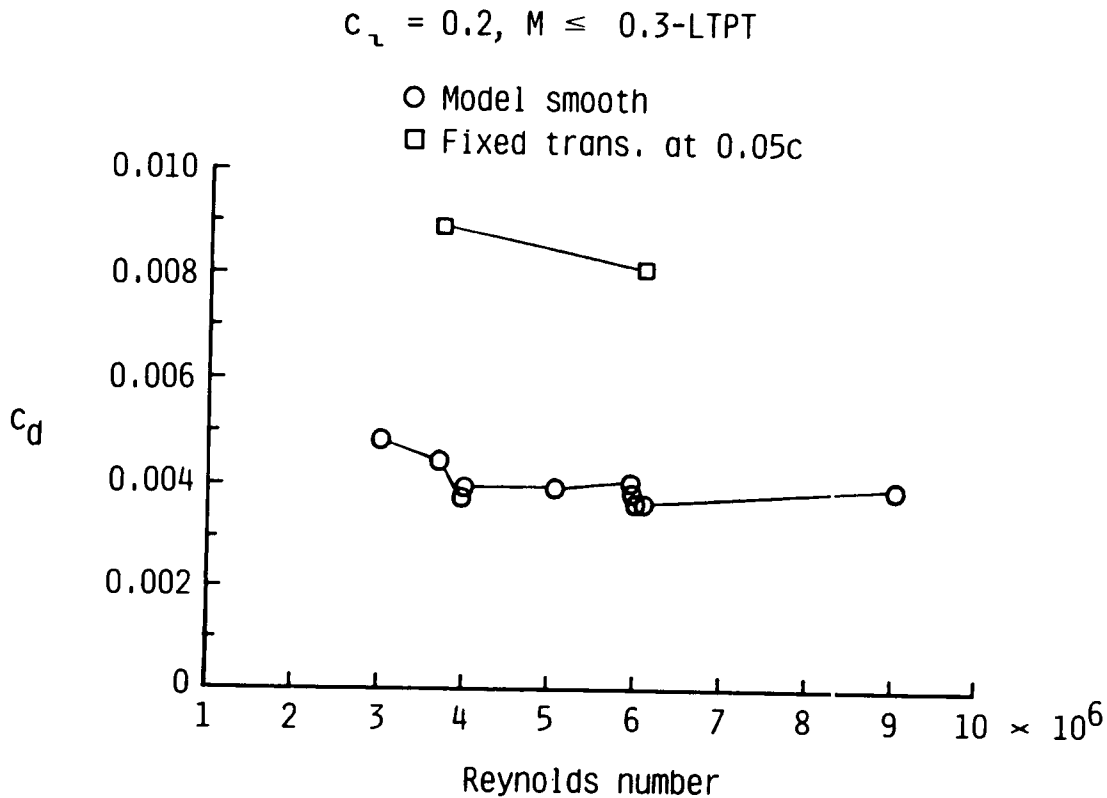


Figure 4

## LOW-SPEED PERFORMANCE

Figure 5 presents the airfoil low-speed performance from the two-dimensional tests in LTPT with the variation of drag coefficient with lift coefficient. The chord Reynolds number is 9 million, and a range of lift coefficients between 0.08 and 0.20 provides the boundaries of the low-drag "bucket".

### HSNLF(1)-0213 AIRFOIL; LTPT DATA

$$R = 9 \times 10^6$$

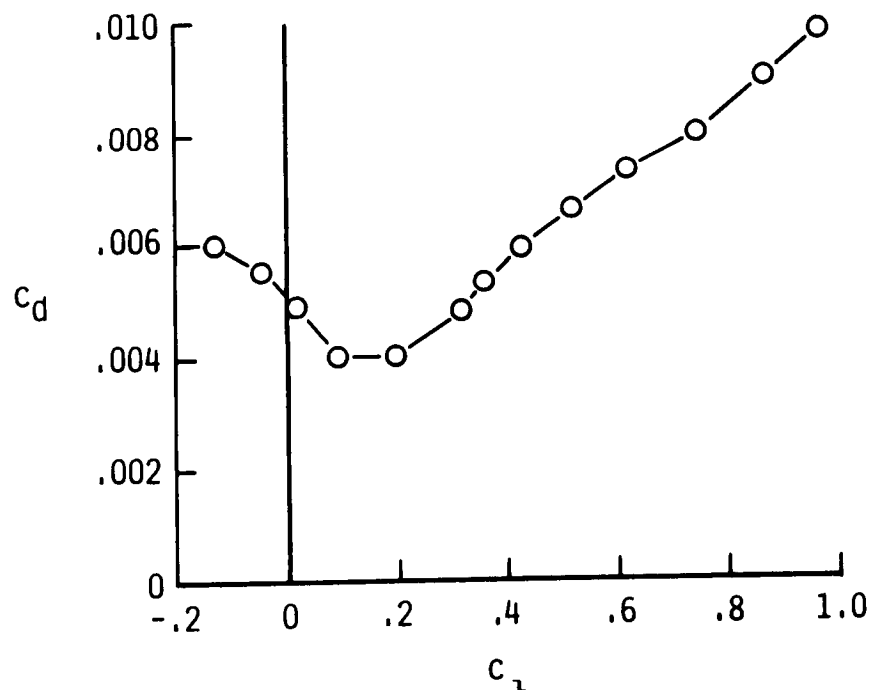


Figure 5



## BOUNDARY-LAYER ASSESSMENT FROM HOT FILM

For the two-dimensional airfoil tests in LTPT, the various states of the boundary layers on the upper and lower surfaces of the model were assessed with hot-film gages. These flush-mounted devices allowed the determination of laminar, transitional, or turbulent flows and were mounted at 30-, 40-, 50-, and 60-percent chord on the upper surface and 40-, 50-, 60-, and 70-percent chord on the lower surface.

Figures 6a and 6b show the states of the boundary layers at these chord stations with varying lift coefficients. Both upper and lower surfaces are presented at Reynolds numbers of 3 and 9 million. The laminar boundary layers, denoted by the open circle symbols, diminish from the upper surface with increasing lift coefficient as the transition location moves upstream. The lower surface responds in the opposite manner by gaining more laminar flow. However, since the highest local flow velocities are on the upper surface, the skin friction for the turbulent boundary layers on the upper surface contributes the net increase in drag with increasing lift coefficient, as seen in figure 5.

At lift coefficients below 0.08, the transition point on the lower surface begins to move forward as lift coefficient decreases, and the drag increases in the same manner as seen for the higher lift coefficients ( $c_l > 0.2$ ).

In several instances, the boundary layers on the same surfaces at the same lift coefficients will have different amounts of laminar flow at the two different Reynolds numbers. These differences are due to the higher turbulence levels in the facility at the higher Reynolds number, which in turn, causes earlier transition.

$$R = 3.0 \times 10^6; M = 0.047 \text{ (LTPT)}$$

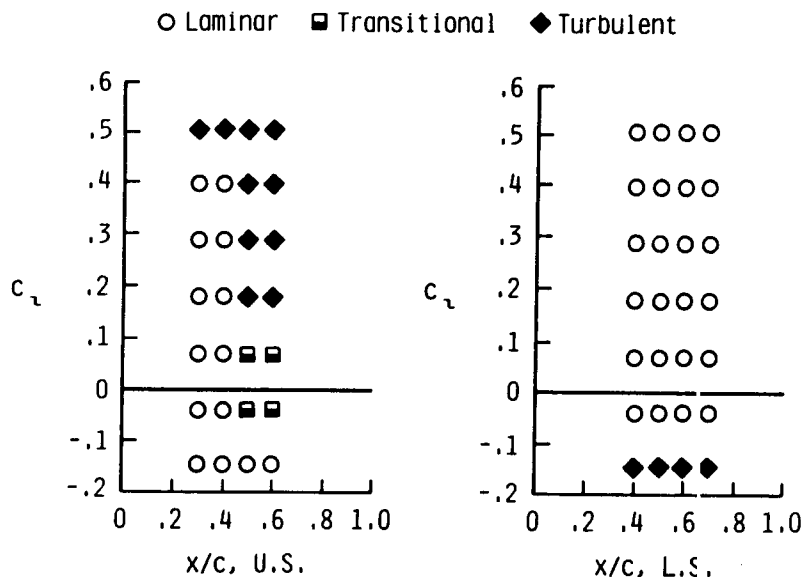


Figure 6a

# BOUNDARY LAYER ASSESSMENT FROM HOT FILM

$R = 9.0 \times 10^6$ ;  $M = 0.139$  (LTPT)

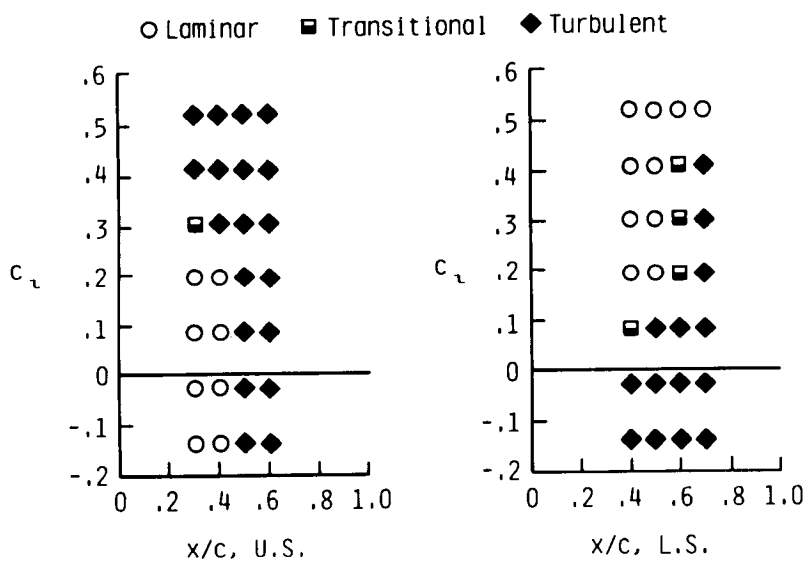


Figure 6b

## MAXIMUM LIFT OF BASIC AIRFOIL

The maximum lift coefficient of the basic airfoil measured in the two-dimensional tests is presented in figure 7. Here, the variation of maximum lift coefficient with Mach number is provided for Reynolds numbers of 3, 4, and 6 million.

At a Reynolds number of 6 million, the maximum lift coefficient appears to decrease by almost 10 percent in value at the highest Mach number. The pressure tunnel allows independent variation of Mach number and Reynolds number to learn the true variation of maximum lift with either of these parameters.

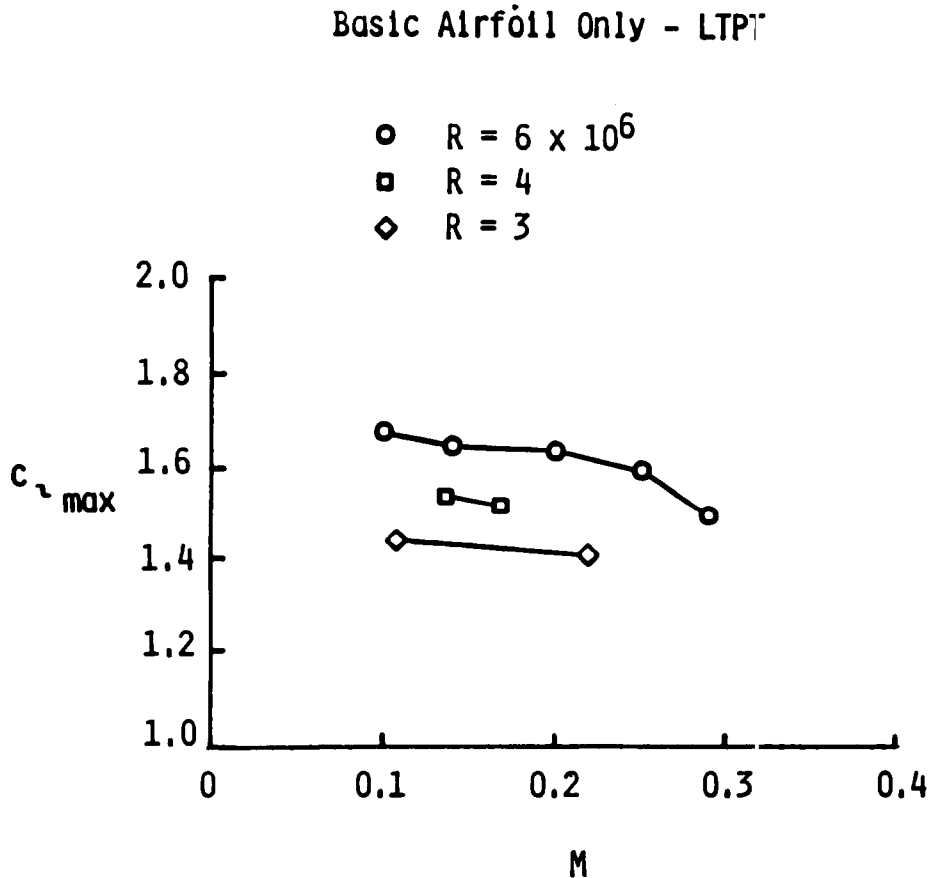


Figure 7

## SPLIT-FLAP PERFORMANCE

To evaluate the capability of a simple high-lift device, a simulated split flap of 0.20 chord length was mounted on the lower surface of the airfoil model in LTPT. The split flap served as a baseline high-lift device in the testing reported in ref. 2 as well as this test.

This flap was deflected 60 degrees, and its effect is shown in figure 8 with the variation of lift coefficient with both angle of attack and pitching-moment coefficient. The split-flap provides a large increase in maximum lift coefficient, from 1.65 to 2.50, but also causes more negative pitching moment.

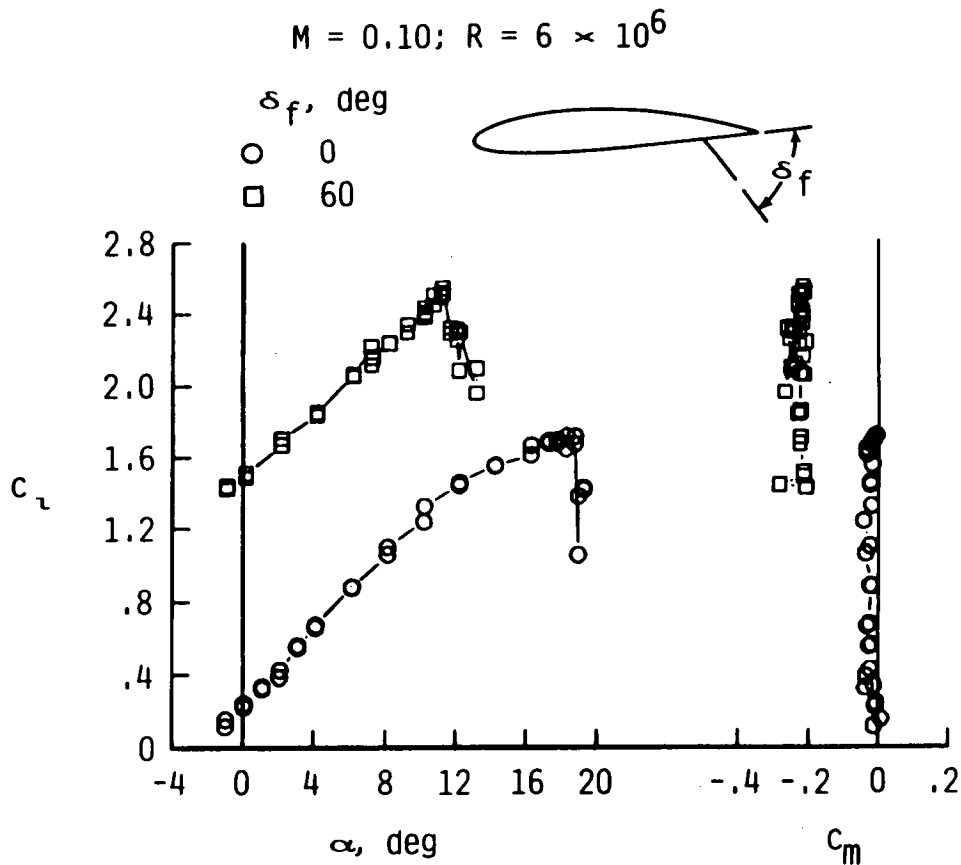


Figure 8

## HIGH-SPEED TESTS IN 6- BY 28-INCH TRANSONIC TUNNEL

Evaluation of the airfoil performance at cruise and climb speeds was provided by two-dimensional tests in the Langley 6- by 28-Inch Transonic Tunnel (6x28 TT). The tests were conducted at Mach numbers ranging from 0.50 to 0.78 and at Reynolds numbers of 4 and 10 million. (Figure 9).

The model for these tests is shown in figures 10a and 10b as a solid shape with routing for chordwise surface pressure measurements. The measured pressure distributions were integrated along the chord to give normal force and pitching moment. Drag was measured by a traversing wake-survey probe.

The 6x28 TT is a blowdown facility and is unsuitable for testing natural laminar-flow airfoils. Drag measurements would therefore exceed the theoretical values by significant increments. However, these tests offered experimental pressure distributions at cruise and climb values of Mach number and Reynolds number which would help verify the airfoil design.

- Chordwise pressure distributions
- Wake survey probe for drag
- Blowdown facility
- Unsuitable for laminar flow

Figure 9

## MODEL FOR HIGH-SPEED TESTS

The two-dimensional, high-speed airfoil tests were conducted on the model shown in figures 10a and 10b. A chordwise row of pressure orifices is located on each surface, and the routing associated with these orifices was located entirely on the lower surface to allow minimum surface disturbances on the upper surface.

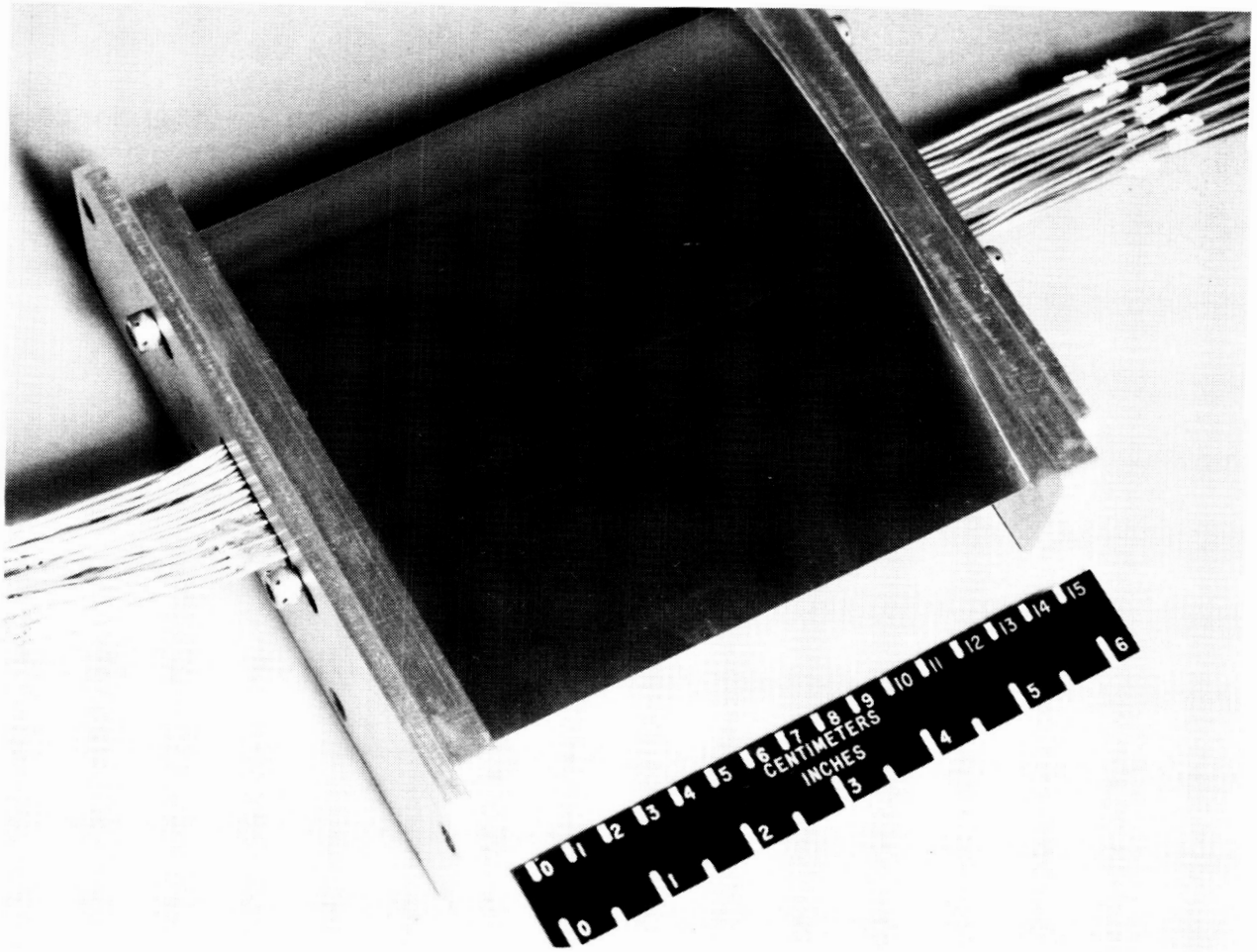


Figure 10a

ORIGINAL PAGE  
BLACK AND WHITE PHOTOGRAPH

~~ORIGINAL PAGE IS  
OF POOR QUALITY~~

~~ORIGINAL PAGE IS  
OF POOR QUALITY~~

MODEL FOR HIGH-SPEED TESTS

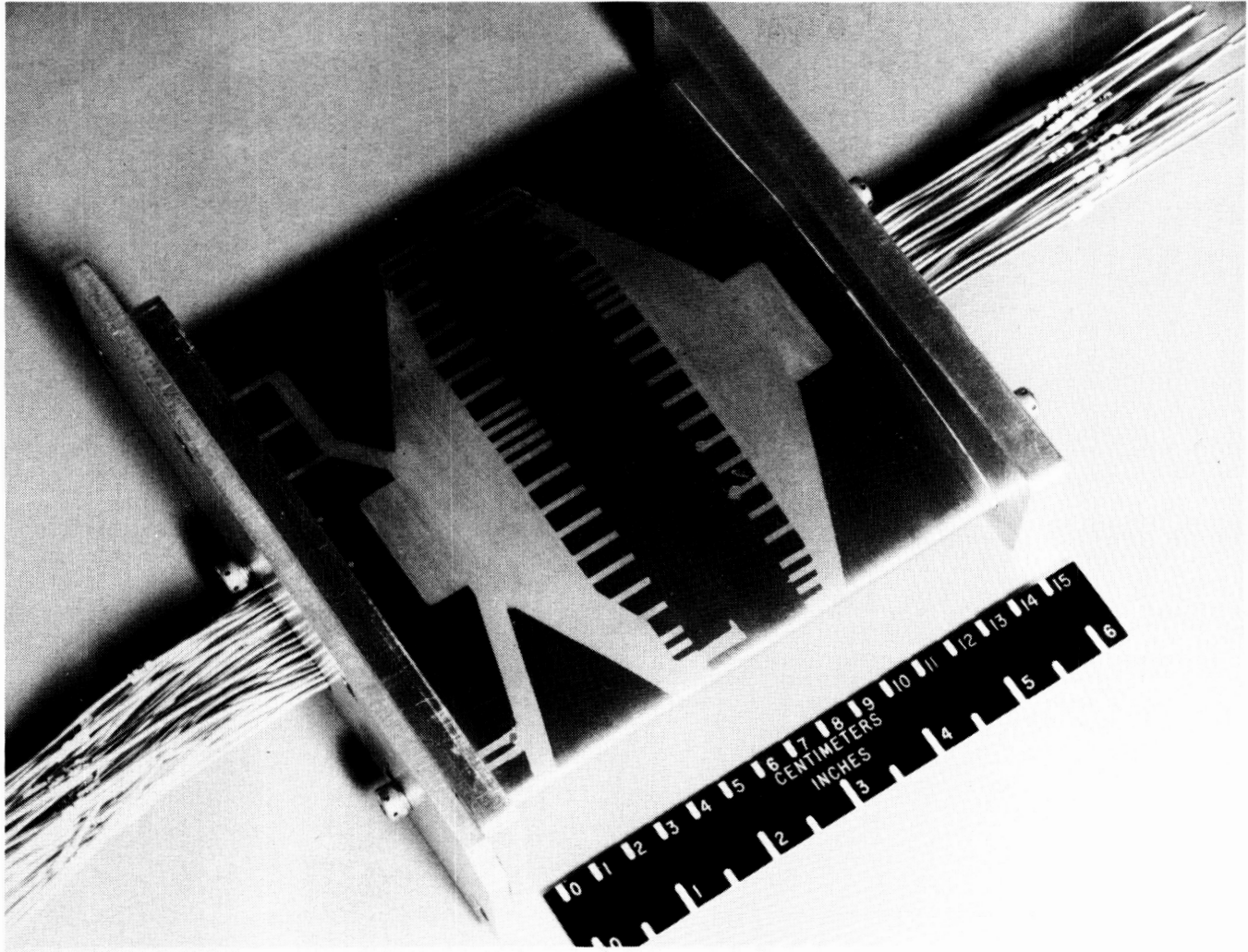


Figure 10b

ORIGINAL PAGE  
BLACK AND WHITE PHOTOGRAPH

## TWO-DIMENSIONAL, HIGH-SPEED RESULTS

Results from the high-speed airfoil tests are shown in figure 11, which consists of the airfoil section characteristics for the smooth model, i.e., free transition, at the design Mach number of 0.70.

The section characteristics are given for three values of Reynolds number, ranging from 4 to 10 million, and indicate essentially identical behavior for the variation of normal-force coefficient with both angle of attack and pitching-moment coefficient.

For normal-force coefficients between 0.25 and 0.30, the drag coefficients at the 4.3 million Reynolds number still remain lower but become somewhat erratic. Drag levels at the 8.6 and 10.4 million Reynolds numbers have similar values to the low-speed data for minimum drag with fixed transition (see figure 4). This behavior indicates sufficient flow quality to allow some laminar boundary layers at the 4.3 million Reynolds number. At the higher Reynolds numbers, the tunnel turbulence level has probably increased to eliminate any substantial laminar flow.

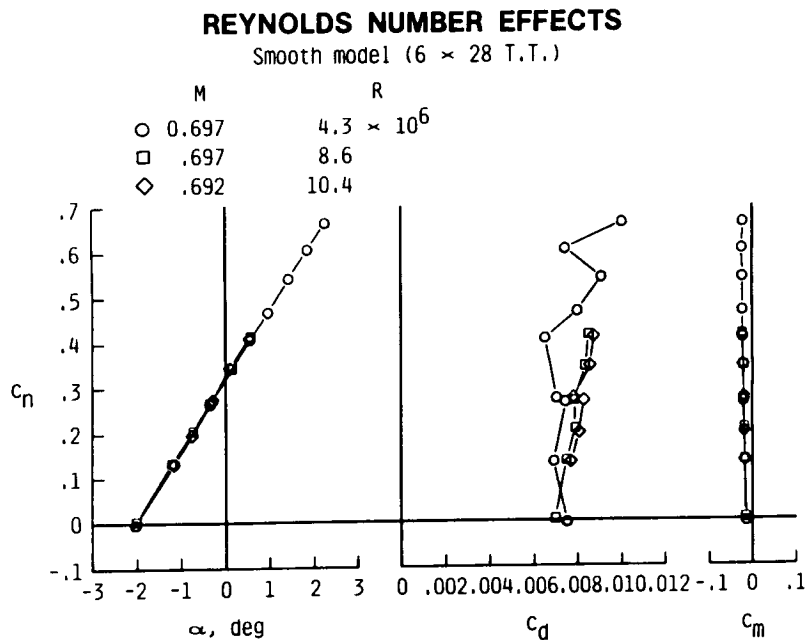


Figure 11



## COMPARISON OF THEORY VERSUS EXPERIMENT

Figure 12 provides a comparison between the high-speed test data and the theory used in the design and analysis of the airfoil (ref. 1). The primary value of this comparison is the close agreement between the experimental and theoretical pressure distributions, which offers a major design verification. Without the proper pressure distribution, the extent of laminar flow on the airfoil would be unachievable.

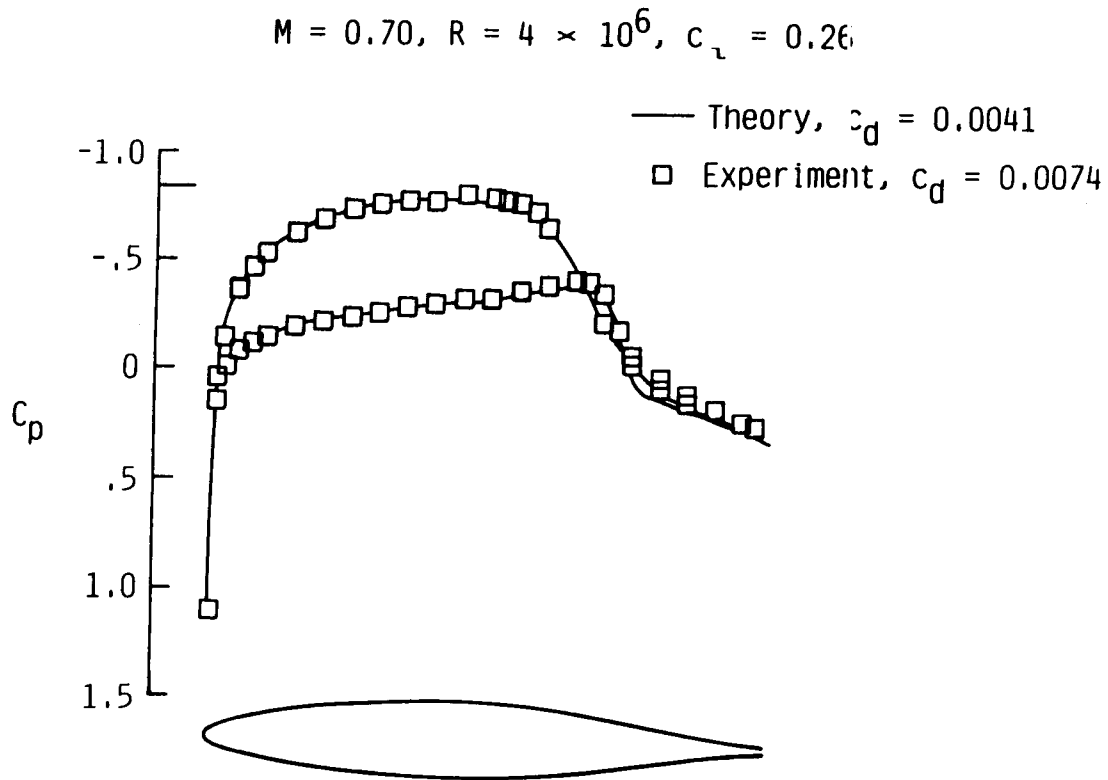


Figure 12

## DRAG-RISE CHARACTERISTICS

Figure 13 illustrates the variation of drag coefficients with Mach number for the high-speed airfoil tests.

Test data were taken with fixed transition at 5-percent chord on upper and lower surfaces to investigate the airfoil performance without laminar flow at the near-design Reynolds number of 10 million. In comparison, the smooth model data at 4 million only had limited amounts of laminar flow due to the tunnel-flow quality.

The important aspects of the drag-rise characteristics in figure 12 are, first of all, that even limited amounts of laminar flow provide an increase in the drag-rise Mach number from 0.72 to 0.74. Also, even without laminar flow, where transition occurs near the leading edge, the drag-rise Mach number for this airfoil still exceeds the design Mach number 0.72 versus 0.70.

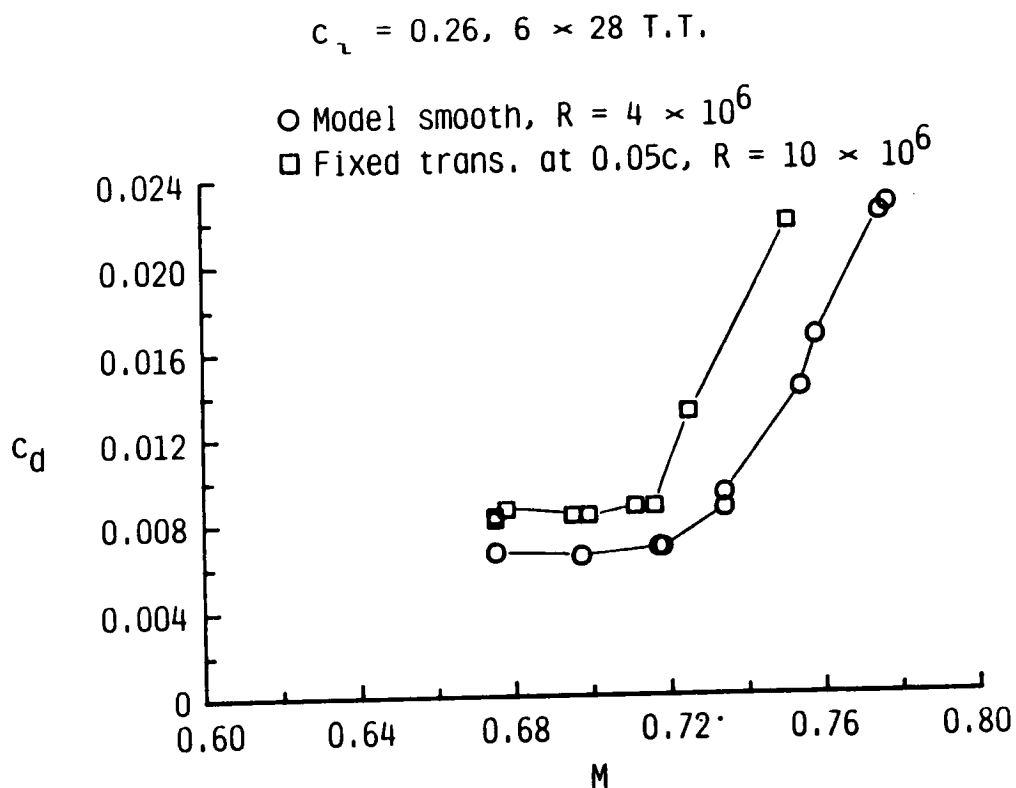


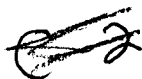
Figure 13

## THREE-DIMENSIONAL TESTS IN 30 x 60 FOOT TUNNEL

Tests of a full-scale, semi-span model using the HSNLF-0213 airfoil section were conducted in the Langley 30- by 60-Foot Tunnel (figures 14a and 14b). The primary purpose was to evaluate the low-speed, high-lift characteristics of a three-dimensional wing using this NLF airfoil section. The tests were conducted at a Reynolds number of  $3.7 \times 10^6$  based on mean aerodynamic chord and over an angle-of-attack range from  $-10^\circ$  to  $30^\circ$ . In addition to force and moment measurements, pressure data, flow visualization, and hot-film data were obtained.

- Full-size semi-span model
- Actual flap system
- Force and moment data
- Hot film and flow visualization

Figure 14a



# SEMI-SPAN MODEL IN THE 30 X 60 TUNNEL

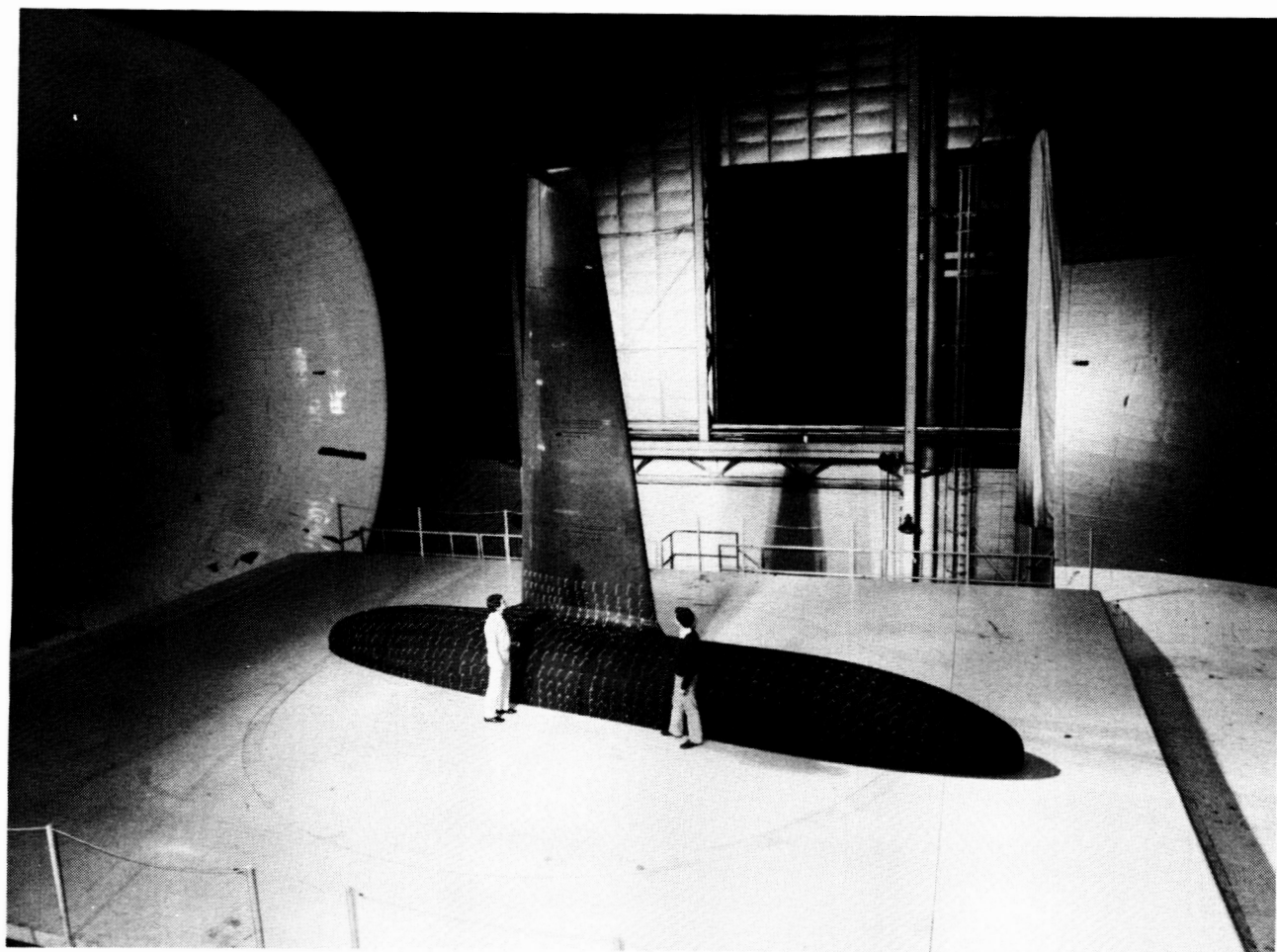


Figure 14b

~~ORIGINAL PAGE IS~~  
~~OF POOR QUALITY~~

ORIGINAL PAGE  
BLACK AND WHITE PHOTOGRAPH

# SEMI-SPAN MODEL GEOMETRY

The model shown in figure 15 includes a body of revolution to simulate the presence of a fuselage near the wing. All force and moment data include the forces and moments acting on the fuselage. The fuselage is representative of a business jet fuselage in size and shape. Also included on the model are a deflectable aileron and spoiler to evaluate roll control and a multi-position flap to determine maximum lift for landing.

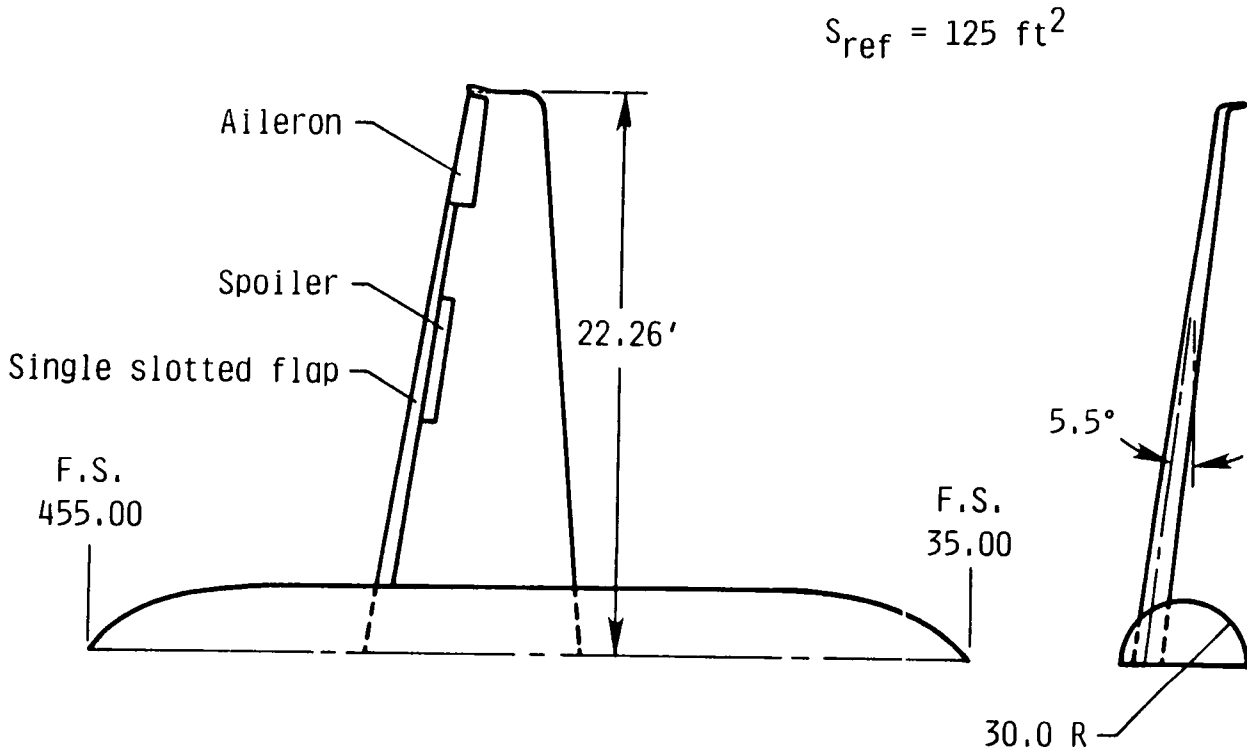


Figure 15

C-2

## SLOTTED FLAP FOR SEMI-SPAN MODEL

Flap deflections are made by changing three brackets located on the lower surface of the wing. Deflections of  $0^\circ$ ,  $5^\circ$ ,  $10^\circ$ ,  $20^\circ$ ,  $30^\circ$ , and  $40^\circ$  are possible. In addition, at the  $40^\circ$  flap deflection, it is possible to vary both the gap and overlap of the flap. The flap is a 28-percent chord flap that extends from the wing root to a span location of  $2y/b = 0.79$ . See figure 16.



Figure 16

~~ORIGINAL PAGE IS  
OF POOR QUALITY~~

ORIGINAL PAGE  
BLACK AND WHITE PHOTOGRAPH

## EFFECT OF FLAP DEFLECTION ON LIFT

The lift characteristics for both  $0^\circ$  and  $40^\circ$  flap deflections are shown in figure 17. With the flap undeflected, a  $C_L$  of about 0.25 is achieved at  $\alpha = 1^\circ$ . This  $C_L$  is close to  $C_L = 0.27$  predicted by the design techniques used in developing the twist distribution for the three-dimensional wing. For the undeflected flap configuration, a  $C_{L_{max}}$  of 1.4 was achieved. Using the optimal gap and overlap settings with  $40^\circ$  of flap deflection increases  $C_{L_{max}}$  to 2.6.

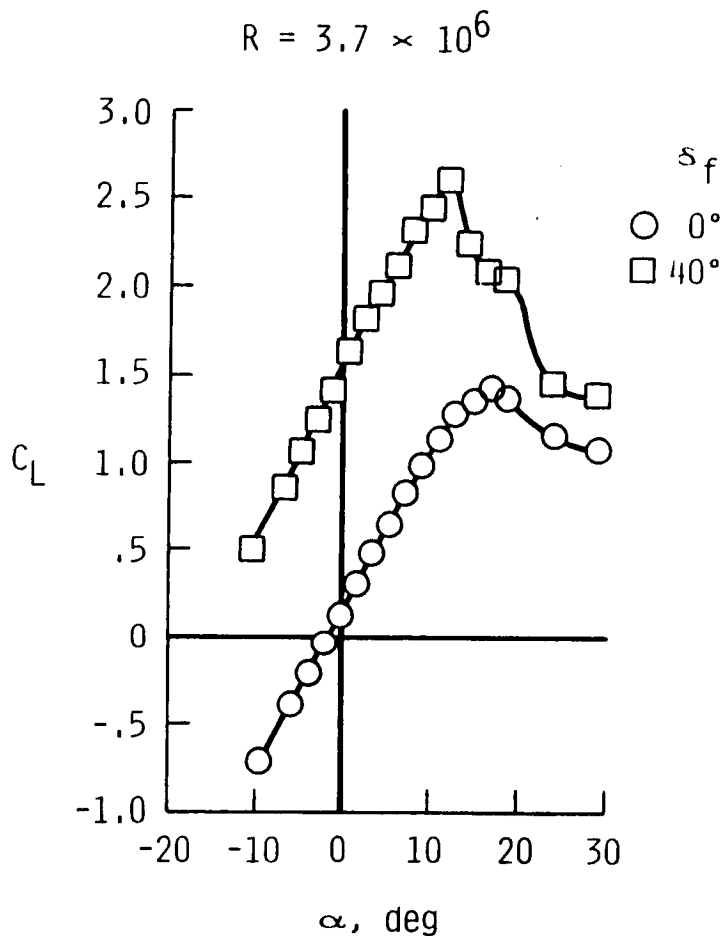


Figure 17

## HOT-FILM GAGE INSTALLATION

In order to obtain data on the amount of laminar flow being achieved on the wing during the tests, six sets of hot-film sensors were placed on the wing (three sets on the upper surface, three sets on the lower surface). These sensors were placed at the 5-, 10-, 20-, 30-, 40-, 50-, 60-, and 70-percent chord locations in such a way that any turbulence generated by a sensor connection would not impact the sensors downstream (figure 18).

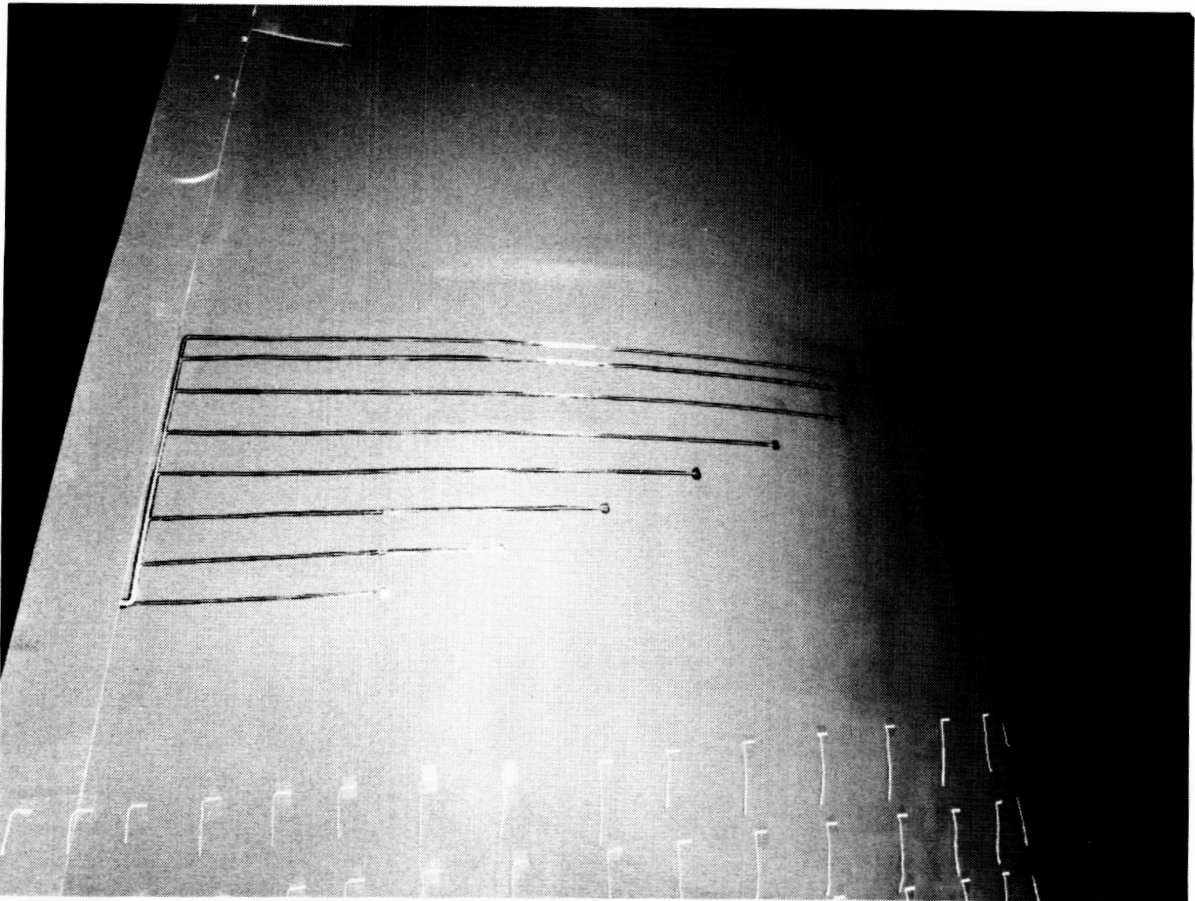


Figure 18

~~ORIGINAL PAGE IS  
OF POOR QUALITY~~

ORIGINAL PAGE  
BLACK AND WHITE PHOTOGRAPH



## REGIONS OF LAMINAR AND TURBULENT BOUNDARY LAYERS

Hot-film data taken at  $\alpha = 1^\circ$  at a Reynolds number of  $3.0 \times 10^6$  are presented in figure 19. The data indicate that the amount of achievable laminar flow increases from the wing root to the tip. Boundary-layer transition starts between 0.15 c and 0.25 c and becomes fully turbulent by 0.5 c to 0.7 c. Comparisons between previous tests results and flight data have indicated that while boundary-layer transition begins at a more forward chord location in the 30- by 60-foot tunnel, the chord station at which the boundary layer is 100-percent turbulent is generally similar.

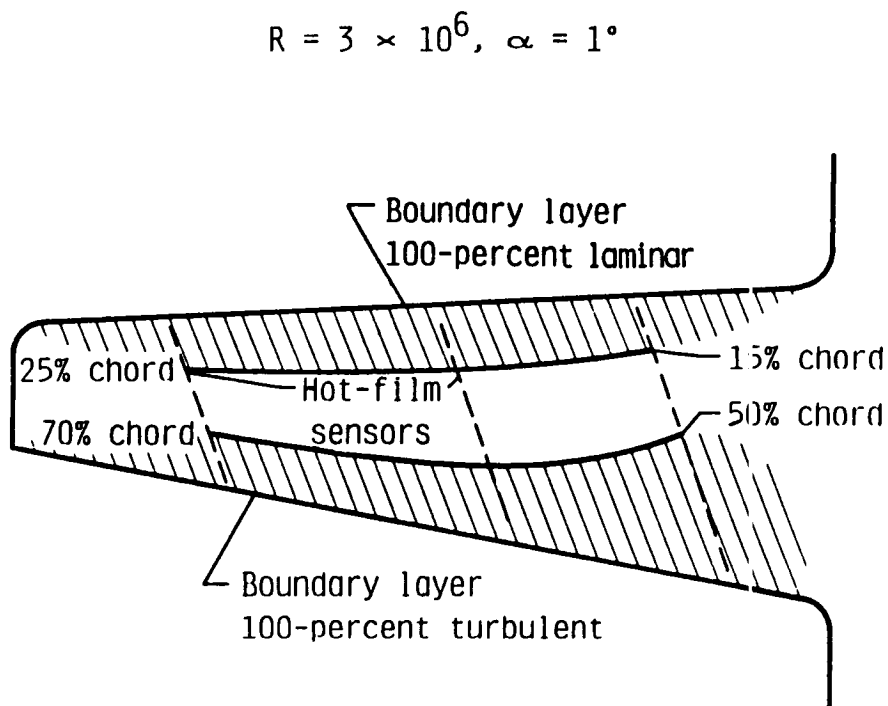


Figure 19

## EFFECT OF BOUNDARY-LAYER TRANSITION ON DRAG

The net result of having a significant amount of laminar flow is a reduction in drag. This result is illustrated in figure 20 where boundary-layer transition was fixed at a chord station near the leading edge of the wing. With transition fixed at  $x/c = 0.05$  on both the upper and lower surface, an increase in  $C_D$  of 0.003 is seen at  $C_L = 0.27$ . Data from two-dimensional tests indicated an increase in  $C_D$  of 0.004 for similar conditions. This difference can probably be attributed to the increased transition band noted earlier in the 30- by 60-foot tunnel data.

$$R = 3.7 \times 10^6 \quad \alpha_f = 0^\circ$$

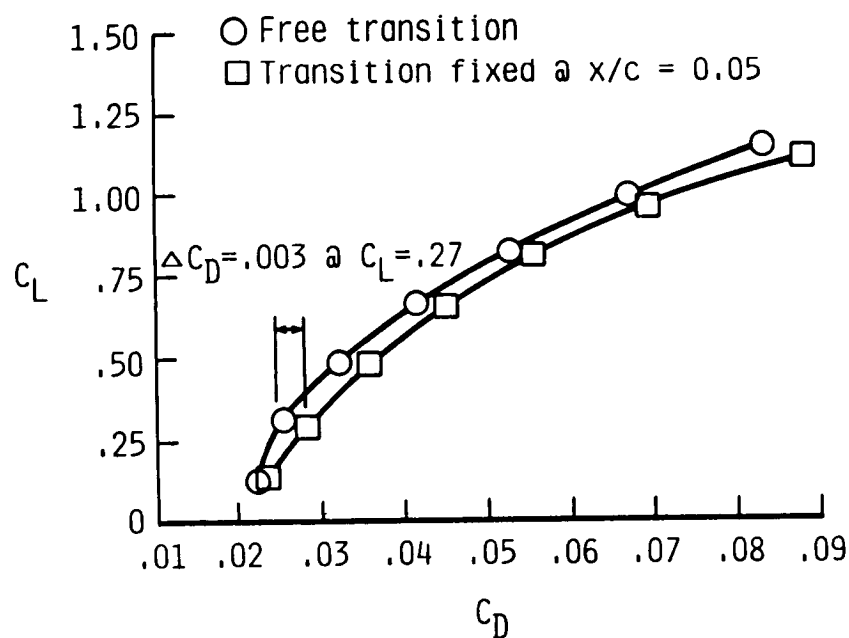


Figure 20

## EFFECT OF BOUNDARY-LAYER TRANSITION ON LIFT

Of final concern is the effect of boundary-layer transition on the lift characteristics, which is shown in figure 21. Ideally, fixed transition would have no effect on lift. Test results, however, usually indicate some negligible reductions in  $C_L$  because of such things as a thickening of the boundary layer or slightly earlier separation than that for the wing with free transition. The data for this airfoil indicate a slight loss in lift near  $C_{L_{max}}$  which is probably due to early separation. This reduction in  $C_L$ , however, is small and its effect on performance would be minimal.

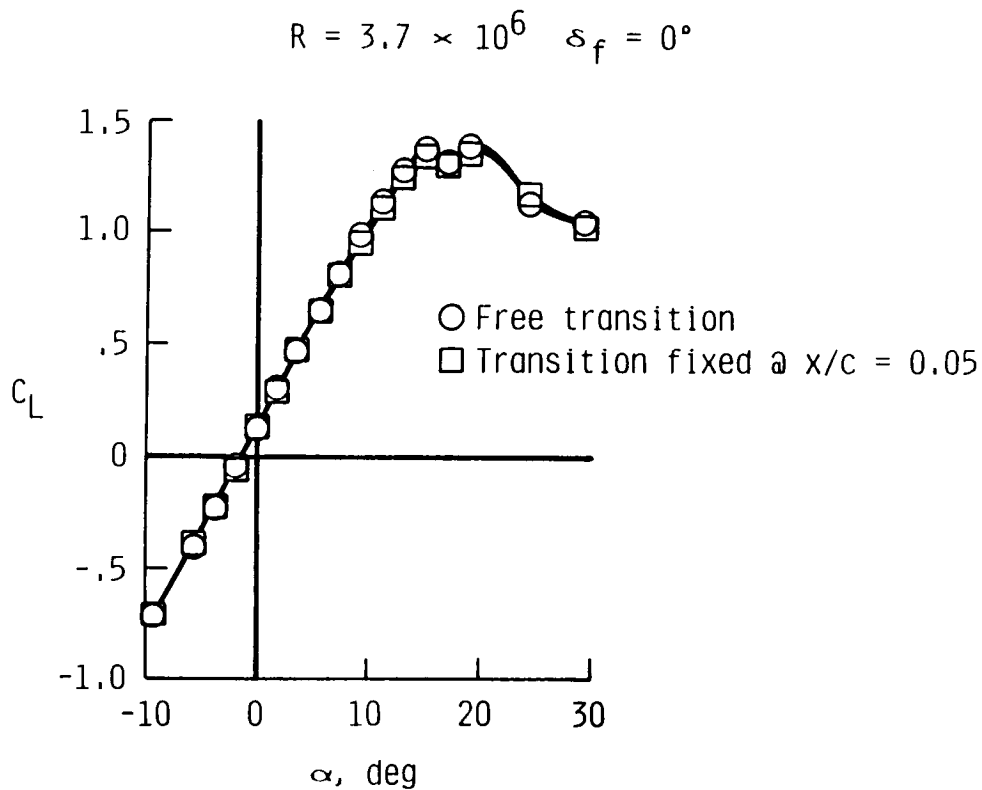


Figure 21

## CONCLUSIONS

The two-dimensional airfoil tests on the HSNLF(1)-0213 airfoil demonstrated the following characteristics during the low-speed and high-speed tests (figure 22):

For the low-speed tests, the hot-film data showed laminar boundary layers back to 40- to 50-percent chord on the upper surface and 50- to 60-percent chord on the lower surface. The conditions for these observations were Reynolds numbers of 9 million, Mach numbers less than 0.30, and lift coefficient of 0.20, which resulted in a drag coefficient value of 0.0040.

The maximum lift in these tests for the basic airfoil ranged from 1.41 to 1.68 at Reynolds numbers of 3 and 6 million, respectively ( $M = 0.10$ ). The simulated split flap increased the maximum lift coefficient to 2.5 at a Reynolds number of 6 million.

The high-speed tests primarily verified the design pressure distribution at the design Mach number of 0.70 and lift coefficient (0.26). In addition, the drag-rise Mach number with fixed transition near the leading edge (0.05 c) still exceeded the design Mach number (0.72 vs. 0.70). For the limited amount of laminar flow achieved with the Reynolds number of 4 million, the drag-rise Mach number increased to 0.74.

Three-dimensional tests on the full-size, semi-span model have evaluated the wing design with a slotted flap to determine the wing maximum lift coefficient and survey the boundary layer along the span. The basic wing (unflapped) obtained a maximum lift coefficient of 1.4 for both free and fixed transition at 0.05 c. With the 40° flap deflection, the maximum lift coefficient increased to 2.5 at the same Reynolds number of 3 million.

At the low angles of attack, hot-film data indicated laminar boundary layers back to 15-percent chord at the inboard station and 25-percent chord at mid-span and outboard stations. The semi-span model has shown drag coefficient values of 0.0030 lower for free transition than for fixed transition at 0.05 c, as compared to the 0.0040 increment observed in the two-dimensional, low-speed tests.

## CONCLUSIONS

- 2-D test results
- Low speed
  - Laminar boundary layers exist on 40%-50% chord u.s. and 50%-60% l.s. with  $c_d = 0.0040$  ( $R = 9 \times 10^6$ )
  - Basic airfoil  $c_{l_{\max}} = 1.44$ ,  $R = 3 \times 10^6$  and  $1.68$ ,  $R = 6 \times 10^6$  for  $M = 0.10$
  - Split-flap  $c_{l_{\max}} = 2.5$ ,  $R = 6 \times 10^6$  for  $M = 0.10$
- High speed
  - Experimental and theoretical pressure distributions match
  - At  $c_l = 0.26$ ,  $M_{\text{drag-rise}} = 0.72$  at  $R = 10 \times 10^6$ , fixed trans.;  
 $M_{\text{drag-rise}} = 0.74$  at  $R = 4 \times 10^6$ , free trans.
- 3-D test results
  - Basic  $C_{L_{\max}} = 1.4$  free or fixed trans.,  $R = 3.7 \times 10^6$
  - Slotted flaps at  $40^\circ$ ,  $C_{L_{\max}} = 2.6$  free or fixed trans.,  $R = 3.7 \times 10^6$
  - Laminar boundary layers on u.s. back to 15% chord inboard, 25% chord mispan and outboard
  - Drag reduction free trans. vs. fixed trans. = 0.0030 3-D vs. 0.0040 2-D

Figure 22

## REFERENCES

1. Waggoner, Edgar G.; Campbell, Richard L.; Phillips, Pamela S.; Viken, Jeffrey K.: Computational Design of Natural Laminar Flow Wings for Transonic Transport Application. Presented at the Langley Symposium on Aerodynamics, NASA CP-2398, vol.II, April 1985.
2. Abbott, Ira H.; Von Doenhoff, Albert E.; Stivers, Louis S., Jr.: Summary of Airfoil Data. NACA TR 824, 1945.